Effects of spatially limited external magnetic fields on short sample tests of large-scale superconductors

Effects of Spatially Limited External Magnetic Fields on Short Sample Tests of Large-Scale Superconductors

Toshiyuki Mito, Nagato Yanagi, Kazuya Takahata, Akifumi Iwamoto, Takashi Satow and Junya Yamamoto
National Institute for Fusion Science (NIFS), 322-6 Oroshi, Toki, Gifu 509-52, Japan

Naoki Hirano
The Graduate University for Advanced Studies, 322-6 Oroshi, Toki, Gifu 509-52, Japan

Abstract—**For short sample tests of large-scale superconductors, it is difficult to get sufficient spatial uniformity using external magnetic fields because of the size limitations of test facilities. The effects of spatially limited external magnetic fields on short sample tests are discussed by comparing the test results for narrow and broad external magnetic fields. We tested short samples of pool-cooled 10 kA class superconductors using two kinds of split coils which are different in bore size. The measured recovery currents for the narrow external field are more than twice those for the broad field. It shows that the insufficient spatial distribution of the external field biases the stability measurements of superconductors.**

I. INTRODUCTION

To design a superconducting conductor for a large-scale superconducting coil, it is necessary to test short samples of a conductor made on a preproduction basis. We can confirm the superconducting properties and stabilities of proposed conductors by short sample tests. However, there are many restrictions for short sample tests of large-scale superconductors. Especially, it is difficult to get sufficient spatial uniformity using external magnetic fields because of the size limitations of test facilities. It is necessary to estimate the effects of spatially limited external magnetic fields on short samples to apply the test results to stability estimates under the real coil condition of uniform field.

II. SHORT SAMPLE TESTS

A. Stability measurements

Fig. 1 shows a cross sectional view of the KISO-4B(S) conductor which is a scaled down model of the KISO-4B conductor. The KISO-4B was a previous candidate for the LHD [1] helical coils. Parameters of the KISO-4B(S) and KISO-4B are listed in Table 1. At first, we measured the stability of the KISO-4B(S) using a short sample test facility with a small split coil of narrow field as shown in Fig. 2. The recovery currents were measured decreasing the sample current after forced quenches using a heater. The measured recovery currents of the KISO-4B(S) were almost the same as the design values calculated from the design value of the conductor resistance (which was not correct, we found later) [2], so we went ahead to short sample tests of the full size conductor KISO-4B using a test facility with a large split coil of broad field [3]. The parameters of both split coils are listed in Table 2. The measured recovery currents for the KISO-4B were lower than expected based on test results of the scaled down model. The degradation of recovery current could be explained from an anomalous enhancement of magneto-resistivity in an aluminum-copper composite [4]-[6].

Then we measured stabilities of the KISO-4B(S) with the test facility of broad field to confirm the true recovery currents. The measured recovery currents using the broad field were half the previous measurements using the narrow field. Fig. 3 shows measured recovery currents for the narrow and broad external fields as a function of central field.

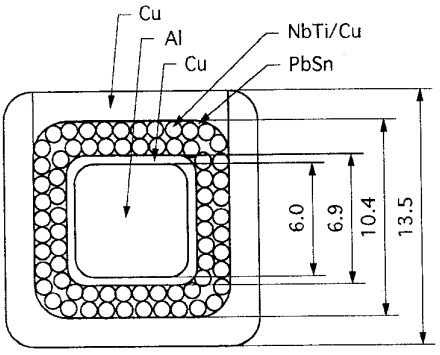

Fig. 1. Cross sectional view of KISO-4B(S) conductor.

TABLE 1
PARAMETERS OF KISO-4B(S) AND KISO-4B

Items	KISO-4B(S)	KISO-4B
Superconductor	NbTi	←
Nominal current	10 kA	21 kA
Size	13.5 mm × 13.5 mm	19 mm × 19 mm
Surface treatment	Copper oxide	←
Critical current (7T)	34 kA	58 kA
Cross section Total	182.3 mm^2	361.0 mm^2
Al	36.0 mm^2	83.4 mm^2
NbTi	21.6 mm^2	38.9 mm^2
Cu	109.8 mm^2	216.9 mm^2
PbSn	14.9 mm^2	25.6 mm^2

TABLE 2
PARAMETERS OF NARROW AND BROAD FIELDS

Items	Narrow field	Broad field
Coil type	Split coil	←
Coil outer diameter	334 mm	907 mm
Coil inner diameter	120 mm	248 mm
Coil length	100 mm	139 mm
Gap width	30 mm	100 mm
Maximum central field	8 T	9 T

Manuscript received June 13, 1995.

T. Mito, mito@nifs.ac.jp, fax 81-572-57-7465, phone 81-572-57-4777;N. Yanagi, K. Takahata, A. Iwamoto, T. Satow, J. Yamamoto, N. Hirano, fax 81-572-57-7465, phone 81-572-57-4777.

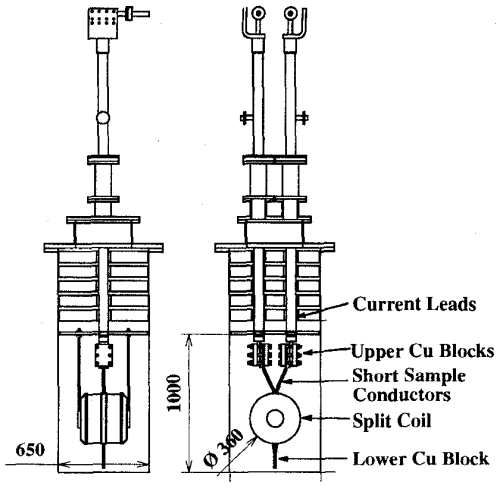

Fig. 2. Short sample test facility with a small split coil of narrow field.

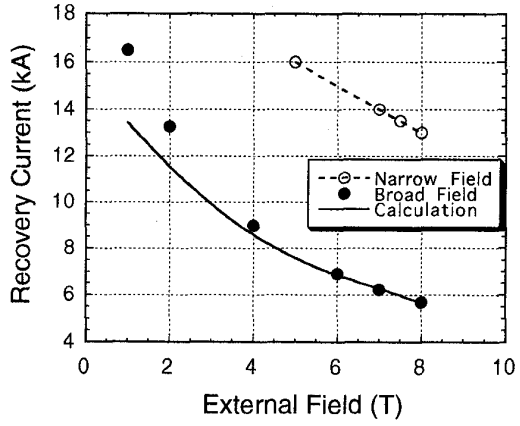

Fig. 3. Measured recovery current under the narrow and broad external fields as a function of central field.

B. Spatial distribution of normal zones

Fig. 4 shows the positions of voltage taps and a heater for short samples with the spatial distributions of the narrow and broad fields. 50% of the conductor surface was covered with GFRP spacers and 50% was cooled with liquid helium. We measured the spatial profiles of the normal zones with voltage taps to investigate variation of recovery current. The generated normal zones stagnated at a sample current slightly larger than the recovery current. Fig. 5 shows the spatial distribution of normal resistances when the normal zone stagnated after forced quenches. There were differences between the narrow and broad fields. The resistances of the broad field were spatially uniform, but those of the narrow field changed spatially. The conductor resistance exceeded the design value because of an unexpected anomalous enhancement of magneto-resistivity in the aluminum-copper composite. The resistances for the broad field were about $3\times10^{-6}\,\Omega$/m. However the resistances for the narrow field ranged from 0.4×10^{-6} to $1.6\times10^{-6}\,\Omega$/m. Therefore the resistances of the broad field were considered the true normal resistance of the conductor but those of the narrow field were the resistances in the current-sharing state when part of current was flowing in the superconductor.

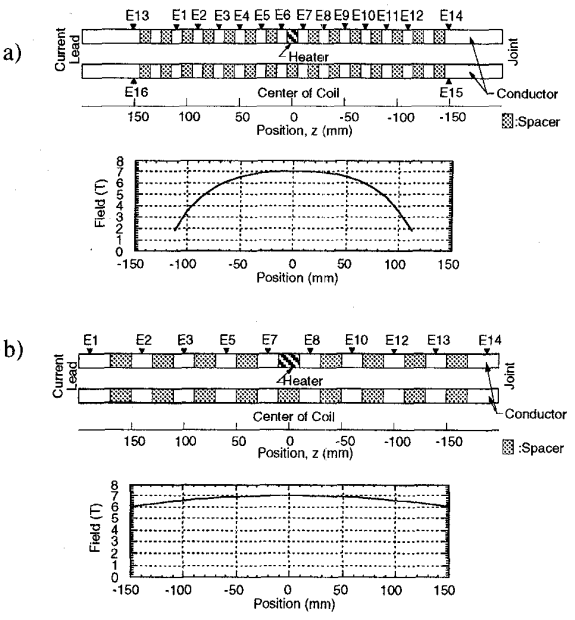

Fig. 4. Positions of voltage taps and heater for short samples with the spatial distribution of a) the narrow field, and b) the broad field.

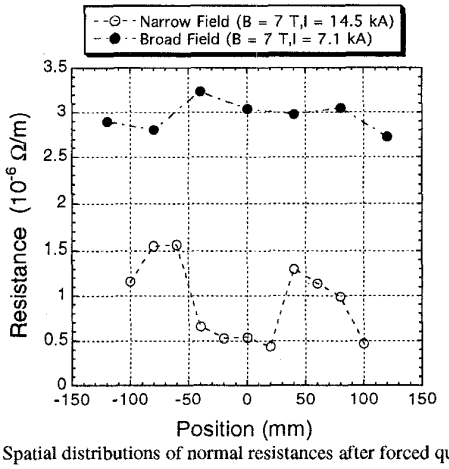

Fig. 5. Spatial distributions of normal resistances after forced quenches.

C. Time variations of normal zone under the narrow field

The normal zone under the broad field reached a plateau as shown in Fig. 5 just after the normal transition, and there was no time variation. Time variations of normal voltages for the narrow field are shown in Fig. 6. There were sharp peaks just after the normal transition, then the voltage signals settled down to constant levels which had the spatial distributions. Changes of the normal zone shapes are shown in Fig. 7 with a parameter of time counted from the onset of heating. The stepwise heat input continued 1 s and the normal zone was generated at 0.96 s just before the end of heat input. At 0.98 s the normal zone had a flat distribution. Then it became hollow at the center and reached a stationary concave distribution after 1.1 s. From the values of the resistances, these normal voltages were considered as the current-sharing state of the superconductor. These voltage distributions at the current-sharing temperature are unstable and transient under the uniform field. However they continued stationary for the spatially restricted narrow-field condition.

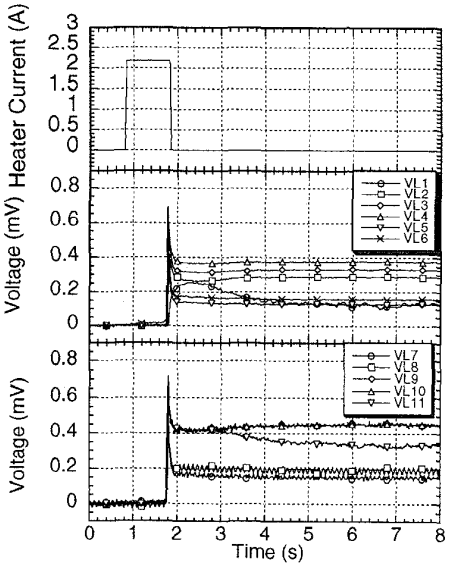

Fig. 6. Time variations of normal voltages for the narrow field.

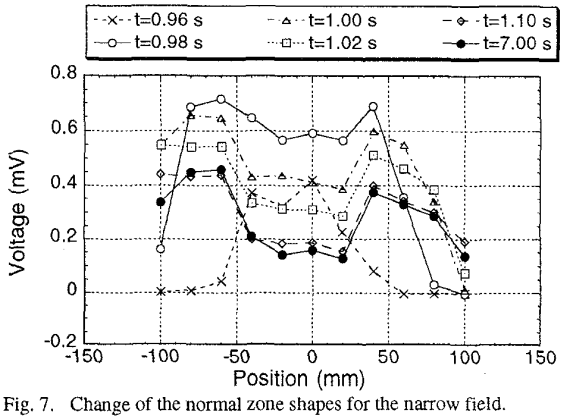

Fig. 7. Change of the normal zone shapes for the narrow field.

III. STABILITY ANALYSES

A. Calculation of cold-end recovery currents

The recovery current was calculated by Maddock's equal-area theorem [7] for the uniform field condition. The cold-end recovery current is defined as a current where the heat transfer to liquid helium balances the heat generation. Then,

$$\int_{T_0}^{T_m} \left\{ Q(T) - \frac{A}{P} G(T) \right\} dT = 0, \qquad (1)$$

where Q is the heat transfer per unit area, G is the heat generation per unit volume, A is the cross-sectional area of the conductor, P is its cooled perimeter, T is the temperature of conductor, T_0 is the bath temperature, and T_m is the cross-over temperature where $Q(T_m)=(A/P)G(T_m)$.

Q(T) is obtained from the measured heat transfer curve and G(T) is calculated from the measured conductor resistance under the broad field. In Fig. 8, Q(T) and (A/P)G(T) for the recovery currents are plotted with a parameter of the external field. The calculated recovery current is shown with a solid line in Fig. 2. Above 4 T the calculated recovery currents agree well with the experimental values for the broad field. The calculated values, however, deviate from the experimental values in the low field region. It is considered that these deviations are due to the effect of the spatially limited external field.

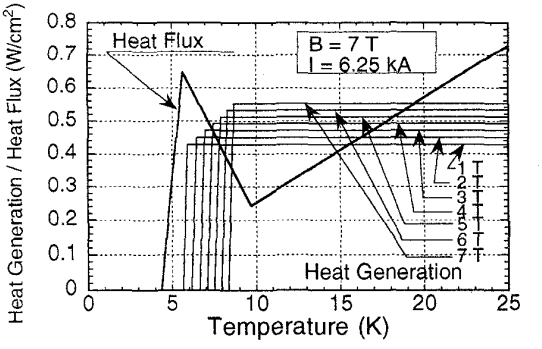

Fig. 8. Heat transfer and heat generation of the conductor as a function of temperature with a parameter of the external field.

B. Calculation of MPZ

To estimate the effect of the spatially limited external field on the recovery current, the minimum propagating zone (MPZ) is calculated using the one-dimensional equation of heat conduction along the conductor [7];

$$Ak(B)\frac{d^2T}{dz^2} = PQ(T) - AG(T), \qquad (2)$$

where k(B) is the thermal conductivity as a function of the external magnetic field B. For simplicity k is assumed to be independent of T.

The values of k(B) are calculated from the thermal conductivities of the individual component materials, then they are revised using a ratio of the resistances calculated from the resistivities of the individual component materials (design values) to the measured resistances, because the anomalous enhancement of magneto-resistivity in an aluminum-copper composite may affect not only resistance but also thermal conductivity. The values of k(B), the design values of resistances, and the measured resistances are listed in Table 3.

The calculated MPZ profiles of the recovery currents are plotted in Fig. 9 with the parameter of the external field. Below 4 T the normal lengths of the MPZ exceed the effective field area of the broad field. This coincides with the deviation point of the measured recovery current under the broad field and the calculated one.

TABLE 3
DATA OF THE CONDUCTOR FOR MPZ CALCULATION

Magnetic field B (T)	Designed resistance (Ω/m)	Measured resistance (Ω/m)	Revised thermal conductivity k (W/m·K)
2	4.37×10^{-7}	1.06×10^{-6}	577
4	5.16×10^{-7}	1.81×10^{-6}	399
6	5.86×10^{-7}	2.55×10^{-6}	321
7	6.01×10^{-7}	2.96×10^{-6}	284
8	6.14×10^{-7}	3.38×10^{-6}	272

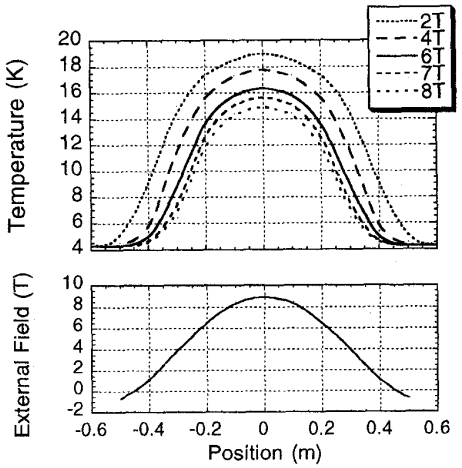

Fig. 9. MPZ profiles of the recovery current as a function of external field.

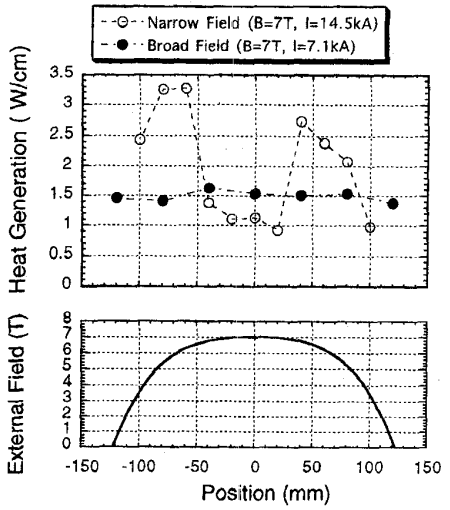

Fig. 10. Spatial distribution of the heat generation for the narrow field with the estimated heat transfer and the conductor temperature.

C. Effects of spatially limited external field

The recovery currents for the spatially limited external field exceed those under uniform field when the effective field length becomes smaller than the MPZ. The recovery currents for the spatially limited external field are calculated as the current where the normal length of MPZ coincides with the effective magnetic field length.

However the increase of the measured recovery current for the narrow field can not be explained by these calculations and is due to some other mechanism.

Fig. 10 shows the spatial distribution of heat generation for the narrow field and the estimated heat transfer and conductor temperatures. The conductor temperatures were calculated from the measured conductor resistances assuming that the conductor was in the current-sharing state. The heat generation coincides with the heat transfer at the center region, which may explain the stationary normal zone at the center. However the heat generation at both edges of the normal zone exceed the heat transfer, and the stable normal zone can not be explained from a one-dimensional study. The mechanisms behind the extraordinary stagnation of the normal zone at the current-sharing temperature are not clear yet. An analysis considering three-dimensional temperature distribution is necessary.

IV. CONCLUSION

The effects of a spatially limited external magnetic field on stability measurements of short sample tests are estimated by comparing test results for narrow, and broad magnetic fields. The measured recovery currents for the broad field were considered correct, and they coincided with the calculated values by Maddock's equal-area theorem when the central magnetic field exceeded 4 T. The measured recovery currents for the broad field below 4 T began to deviate from the calculated values because the MPZ exceeded the effective field length.

The increase of the measured recovery current for the narrow field much less than the MPZ can not be explained using one-dimensional analyses but requires an analysis considering the three-dimensional temperature distribution.

ACKNOWLEDGMENT

The authors are indebted to Prof. A. Iiyoshi, Director General of NIFS, for his continuous encouragement. The authors are also grateful to Prof. R. Tobler for his helpful suggestions.

REFERENCES

[1] O. Motojima, K. Akaishi, K. Fujii, S. Fujiwara, S. Imagawa et al, "Physics and engineering design on the Large Helical Device." *Fusion Engineering and Design*, Vol. 20, 1993, pp. 3-14.

[2] T. Mito, J. Yamamoto, K. Takahata, N. Yanagi, O. Motojima and LHD design Group, "Development of superconducting conductors for Large Helical Device." *IEEE Trans. Magn.*, Vol. 27, No. 2, 1991, pp. 2224-2227.

[3] T. Mito, K. Takahata, N. Yanagi, S. Yamada, A. Nishimura, M. Sakamoto and J. Yamamoto, "Short sample tests of full-scale superconducting conductors for Large Helical Device." *IEEE Trans. Magn.*, Vol. 28, No. 1, 1992, pp. 214-217.

[4] H. Kaneko, "Hall current in aluminum-copper composite." *Advances in Cryogenic Engineering.*, Vol. 40, 1994, pp. 451-458.

[5] N. Yanagi, T. Mito, K. Takahata, M. Sakamoto, A. Nishimura, S. Yamada, S. Imagawa, S. Yamaguchi, H. Kaneko, T. Satow, J. Yamamoto, O. Motojima, "Experimental observation of anomalous magneto-resistivity in 10-20 kA class aluminum-stabilized superconductors for the Large Helical Device." *Advances in Cryogenic Engineering.*, Vol. 40, 1994, pp. 459-468.

[6] S. Imagawa, N. Yanagi, T. Mito, T. Satow, J. Yamamoto, O. Motojima, "Analysis of anomalous resistivity in an aluminum stabilized superconductor for the Large Helical Device." *Advances in Cryogenic Engineering.*, Vol. 40, 1994, pp. 469-477.

[7] M. N. Wilson, *Superconducting Magnets*, Oxford University Press., 1983.